Linear Machine Eddy Current Braking Techniques

BENAROUS, M. * **EASTHAM, J, F.**
TRW Aeronautical Systems EnigmaTEC Ltd., UK
Lucas Aerospace, UK

PROVERBS, J FOSTER, A
Force Engineering Ltd., UK

*The work for this paper was done when working for Force Engineering Ltd

List of principal symbols

f = Supply frequency, Hz
ω = $2\pi f$
μ_0 = Permeability of free air
μ_r = Relative permeability
K_p = Total number of pole pairs around the machine
λ = Wavelength of applied field, m
q = Number of pole pairs in the excited region
A = Magnetic vector potential
M = Magnetic moment distribution
r = Harmonic number
H_c = Permanent magnet coercive force, A/m
t_m = Magnet thickness, m
$spce$ = Spacing between successive magnets, m

Abstract

The analysis of linear machine eddy current brakes is investigated. Two methods are described namely layer-theory and two-dimensional finite element modelling. Both methods are employed for three cases namely A.C supplied linear induction in the plugging and generating mode, linear induction machine with D.C injection and permanent magnet array. The results are validated against experimental test figures obtained from a rotating drum rig and good correlation is obtained for both methods.
The finite element method is useful for final design calculations whilst the layer-theory gives quick answers for initial design and operational calculations.
Key words: Linear eddy current brake, modelling.

1 Introduction

Systems using linear machines as drive elements frequently need to provide braking forces. Linear induction machines can produce retarding forces under the following conditions:

- Plugging
- Regeneration
- D.C. injection

In addition, using permanent magnets to replace the coils supplied with D.C. current can produce the effect of D.C. injection. This paper concentrates on the commonly used reaction plate structure in which a conducting plate is backed by steel. There are a number of papers describing analytical techniques which could be adapted for the situation for example [1] and [2] use Fourier methods for non-magnetic reaction members co-operating with primary using mounted magnets. These and a number of other studies neglected the reaction field produced by the eddy currents. Another recent paper [3] describes a technique for non-magnetic reaction plates, which neglects skin effect. It is the object of this paper to present and validate using a rotating rig the use of two techniques namely 2D layer theory [4] and 2D finite element theory [5] to analyse the problem of linear brakes using steel backed aluminium reaction plates. In both cases the effect of the transverse edges is accounted for using a factor derived from reference [6]. These theories are simple to apply and do not need to make any assumptions relating to skin depth or plate eddy current reaction fields.

2. Braking methods

2.1 Linear Induction Machines:

Plugging: Here the direction of the field is in the opposite direction to the motion. This can be arranged by changing the phase sequence of the machine connections as shown in figure 1. The part of the force speed curve used is indicated in figure 2a

Regeneration: In machine supplied from a variable frequency source the field speed can be arranged to be less than the speed of the wound primary. This produces negative slip and a retarding force. The section of speed force curve used is shown in figure 2a

D.C Injection: Here the primary windings are supplied from a D.C source and a field that is stationary with respect to the primary is produced. The relative velocity between the stator and rotor is zero at standstill and is given by the speed of the moving member under other conditions. This means that the behaviour of the machine about standstill is approximately the same as its behaviour about synchronous speed when A.C currents supply the primary. This is shown in figure 2b

2.2 Permanent Magnet Array

Stationary fields equivalent to those in the D.C. injection case can be produced by an array of alternate polarity permanent magnets. However in this case the

braking cannot be controlled because the magnet mmf cannot be varied.

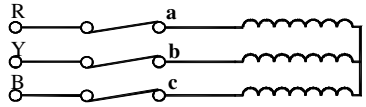

a) Forward

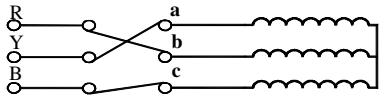

b) Plugging

Figure 1

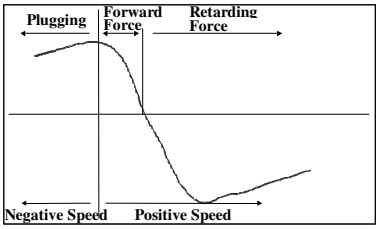

Figure 2a

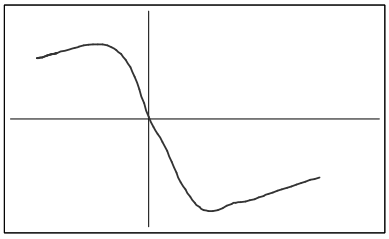

Figure 2b

3 Mathematical Modelling

3.1 Layer Theory

The idealised structure considered comprises a number of laminar regions parallel to the air-gap and of finite extent in the plane of lamination and of arbitrary thickness. Some or all these regions may be conducting and / or ferromagnetic with constant permeability.

The excitation is modelled by an applied current sheet at the interface between two layers, using sinusoidal distribution along the plane of lamination and with the current flowing normally to the direction of motion. This model is shown in figure 3.

Figure 4 shows the equivalent circuit for the machine developed from the above model. Here the impedances are given by Z_A and Z_B [7]. For a region n, the impedances are given by:

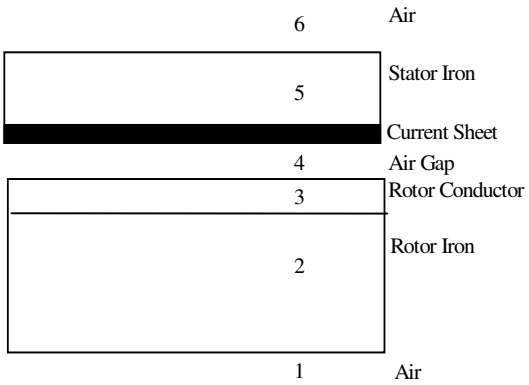

Figure 3 Model for the different regions

$$Z_{A,n} = Z_n^{'} \tanh\left(0.5\,\gamma_n\, S_n\right)$$
$$Z_{B,n} = Z_n^{'} \Big/ \sinh\left(\gamma_n\, S_n\right) \qquad (1)$$

Where $Z_n^{'} = j\omega\mu_0\mu_{y,N} \,/\, \gamma_n$ (2)

And $\gamma_n = \left(k^2 + j/d_n^2\right)^{1/2}$ (3)

$$d_n = \left(\rho_n/\mu_0\mu_n\,\omega_n\right)^{1/2}$$

The form of the applied current sheet required from a linear motion is found from figure 5, the stator excitation extends between $-q\pi/K_p$ and $+q\pi/K_p$ radians, and has the form

$$\hat{J}_s \sin\left(\omega t - K_p\, x_1\right) \qquad (4)$$

Using Fourier analysis, this excitation can be represented by

$$J_s = \sum_{n=-\infty}^{+\infty} J_{1n} \qquad (5)$$

Where $J_{1n} = \hat{J}_{1n} \sin\left(\omega t - n x_1\right)$

$$\hat{J}_{1n} = A_{1n}\,\hat{J}_s$$

$$A_{1n} = \frac{q}{K_p}\frac{\sin\alpha n}{\alpha_n}$$

and $\alpha_n = \left(n - K_p\right)\dfrac{q\pi}{K_p}$

The effect of the longitudinal edges is accounted for by using an assembly of the harmonics found from the analysis of a short section of excitation on the circular equivalent model [8]. The test linear motor was analysed for different braking and drive modes using this technique and the results are shown in figure 6.

In addition the situation using permanent magnets instead of D.C current fed windings was analysed.

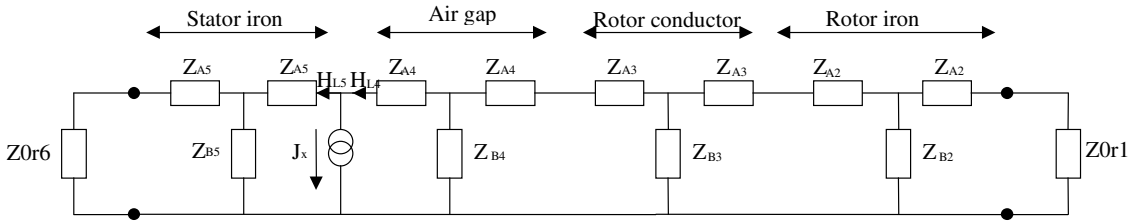

Figure 4 Equivalent circuit Impedance network

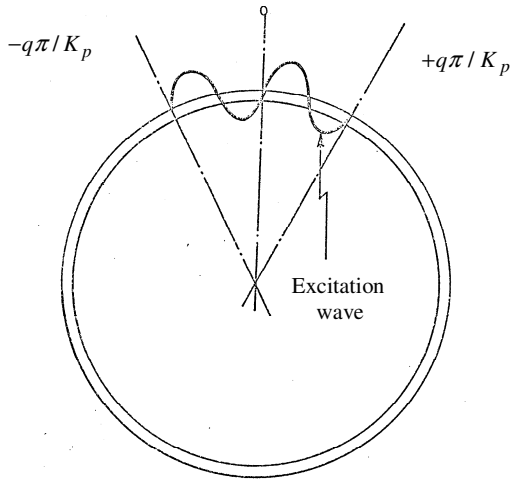

Figure 5 Excited region

Figure 7 shows the results obtained for a LIM in a D.C. injection brake mode with only two phases energised by connecting a voltage source across two of the input terminals. Figure 8 shows the results for the permanent magnet brake described in the appendix.

The magnets were modelled with the perimeter coils having ampere-turns given by $H_c l_m$. The effect of these was found by the use of multiple thin layers as shown in figure 9. Whilst this region could have been treated using a thick excitation layer [8] it is convenient simply to set up an iterative loop in the model.

The current loading expression is defined as:

$$J_s = \sum_{r=1}^{\infty} \frac{2}{\sqrt{2}} H_c t_m T_{\Pr} \cos\left(r * spc * \pi / (2 * T_P)\right) \qquad (6)$$

and $$T_P = T_{\Pr} / r$$

3.2 2D Finite Element Analysis

Many devices can be reasonably modelled using 2D finite element methods, providing it can be assumed that the field does not change in some direction. This is the Z direction in the model. The formulation solves for a single component of the magnetic vector potential [10], $\mathbf{A} = A_z \hat{\mathbf{Z}}$. The field quantities are derived from $\mathbf{A}$. The induced e.m.f is,

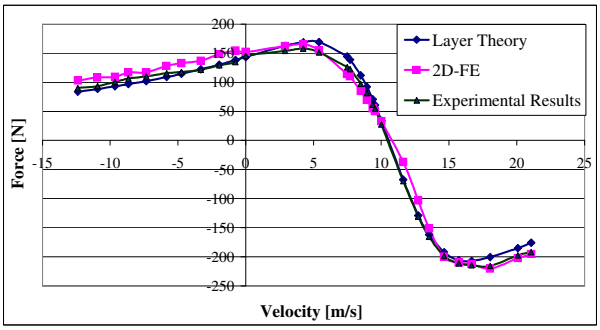

Figure 6 LIM AC supplied: predicted and measured force

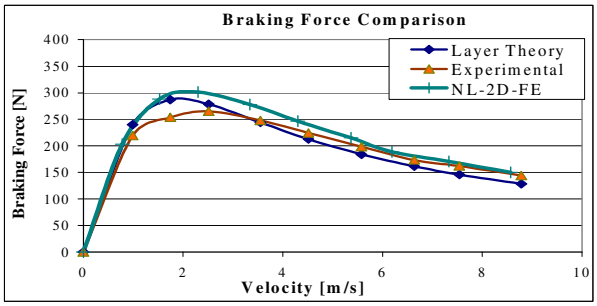

Figure 7 LIM D.C injection: predicted & measured force

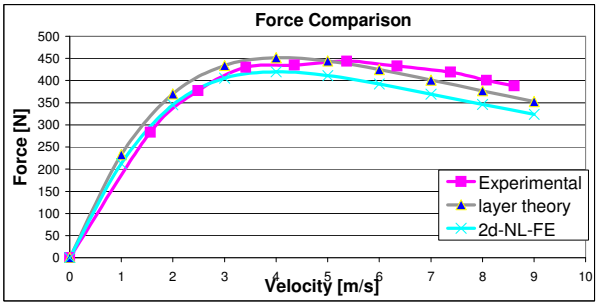

Figure 8 Permanent magnet: predicted & measured force

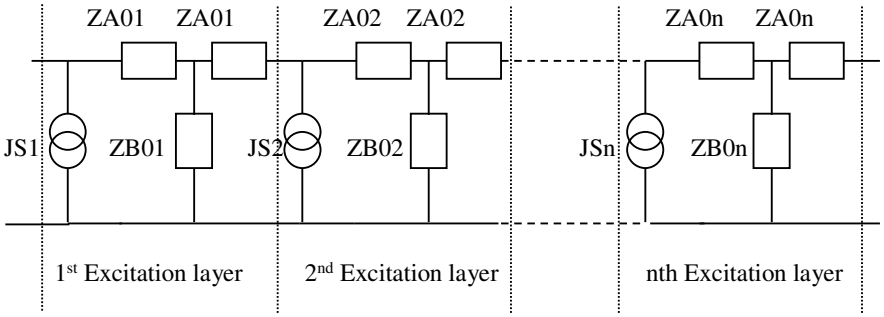

Figure 9 Multiple thin Layers for the permanent Magnet

$$E_Z = -\frac{\partial A_Z}{\partial t} \qquad (7)$$

and the magnetic flux density is,

$$\mathrm{B} = \nabla \times \mathrm{A}_Z \hat{\mathrm{Z}} \qquad (8)$$

The governing partial differential equation is deduced from Maxwell's equation, substituting into $\nabla \times \mathrm{H} = \mathrm{J}$ gives,

$$\nabla \times \frac{1}{\mu} \nabla \times A + \sigma \frac{\partial A}{\partial t} = J_S \qquad (9)$$

Which reduces to

$$-\nabla \cdot \frac{1}{\mu} \nabla A_Z + \sigma \frac{\partial A_Z}{\partial t} = J_S \qquad (10)$$

Equation (10) shows that the current is described by two terms, one due to the induced eddy currents and a second prescribed source current term. In the linear induction machine model wound coils are to be used, then the current density is simply the current flowing in a turn, $\mathbf{I}_{coil}$, times the number of turns per square meter, **t**. Where t is a vector quantity because there is a direction (in or out) associated with it.

$$\mathbf{J} = \mathrm{I}_{coil}\, \mathbf{t} \qquad (11)$$

Coils are connected to an external circuit. The voltage on the coil terminals is found by integrating the induced e.m.f. over the coil region, for a 2 dimensional problem with device length, l, we obtain,

$$V_a = l \int t \cdot \dot{A}\, dS \qquad (12)$$

The equations to be solved are now,

$$-\nabla \cdot \frac{1}{\mu} \nabla A_Z + \sigma \frac{\partial A_Z}{\partial t} - tI_{coil} = 0 \qquad (13)$$

$$\int \sigma t \frac{\partial A_Z}{\partial t} dS - V_a = 0 \qquad (14)$$

In the same way as described earlier the conductivities of the regions are modified according to [5].

3.2.1 Permanent Magnets

In 2D FE permanent magnets are treated as magnetic moment distribution [9], the magnetic flux density is thus defined as:

$$B = \mu_0 \left(H\, \mu_r + M \right) \qquad (15)$$

Alternatively in terms of the remnant flux density, B_{rem},

$$B = \mu_0\, \mu_r\, H + B_{rem} \qquad (16)$$

Using the remnant flux density formulation in equation (9) gives:

$$\nabla \times \frac{1}{\mu} \nabla \times \mathrm{A} + \sigma \frac{\partial \mathrm{A}}{\partial t} = J_s + \nabla \times \frac{1}{\mu} B_{rem} \qquad (17)$$

The above analysis was used to predict the performance of the A.C supplied linear induction machine, the linear induction machine with D.C injection and the permanent magnet brake. Appropriate graphs are plotted in figures 6, 7 and 8.

3.2.2 Moving Conductor problems

Many problems involve moving conductors. If such conductors have a constant cross-section normal to the direction of motion and the velocity is constant then it is possible to use the Minkowski transformation to solve the problem [6]. The equation to be solved is:

$$\nabla\times\frac{1}{\mu}\nabla\times A+\sigma\frac{\partial A}{\partial t}-\sigma v\times\nabla\times A=0 \qquad (18)$$

Which for 2D Cartesian problems reduces to:

$$-\nabla.\frac{1}{\mu}\nabla A_z+\sigma\frac{\partial A_z}{\partial t}-\sigma v\times\nabla\times A_z\hat{z}=0 \qquad (19)$$

Figure 10 shows the flux plot obtained at zero speed from the above analysis. It will be observed that the detailed geometry is preserved and that the method unlike the layer theory can be used for detailed design of tooth and backing iron flux densities.

4 Test Rig

The drum rig used for experiments is shown in figure 11, while figure 12 represents the permanent magnet arch unit used in permanent magnet brake mode

In the case of plugging, regeneration, and D.C injection the arch supporting the permanent magnet set is replaced by a linear induction motor. The D.C injection tests were done with only two of the motor three phase windings connected in series, and fed from a D.C power supply.

The results obtained were corrected to allow for the effect of the arc and are shown at figures 6, 7 and 8 together with the values calculated from both layer theory and finite element methods.

5 Conclusions

The paper has used two easily applied modelling techniques namely layer theory and 2D finite element theory to the modelling of linear eddy current brakes.

Experimental results have been presented which show good correlation between theory and practice for the configuration considered namely:

- A.C supplied machine
- D.C injection
- permanent magnets

The accuracy of the results in all cases is easily good enough for design purposes.

Both of the analytical techniques can be freely applied to machines of any dimensions since skin depth and eddy current reaction fields are fully accounted for. However the difference in computation time between the finite element and the layer theory modelling is considerable. A single point on one of the graphs take of the order of 15 minutes, whereas using the same computer a whole curve of a layer theory plot, say 10 points takes only 1 minute. The virtue in finite element modelling lies in the exact calculation of tooth and backing iron flux which can only be found very approximately using the layer theory. Thus finite element modelling is best used for final electromagnetic design work whilst layer theory gives quick results for initial design and operational results.

6 References

[1] Nagaya, and Y.Karube, “A rotary eddy current brake or damper consisting of several sector magnets and a plate conductor of arbitrary shape” IEEE Trans. Magn, 1987. 23. pp 2136-2145.

[2] K.Nagaya, H.Kojima, Y.Karube, and H.Kibayashi, “Braking forces and damping coefficients of eddy current brakes consisting of cylindrical magnets and plate conductors of arbitrary shape” IEEE Trans. Power Appar. Syst. 1984. 20. pp 21236- 2145.

[3] J.D.Edwards, B.V.Jayawant, W.R.C. Dawson, and D.T. Wright. “ Permanent-magnet linear eddy-current brake with a non-magnetic reaction plate” Proc.IEE, Vol. 146, No. 6, November 1999, pp 627-631

[4] J.Greig, and E.M.Freeman, “Travelling-wave problem in electrical machines” Proc.IEE, Vol. 114, No. 11, November 1967, pp 1681-1683

[5] J.F.Eastham, R.Akmese, D.Roger, and R.J.Hill-Cottingham, “Prediction of thrust forces in tubular induction machines.” IEEE Trans. Magn., MAG 28(2): March 1992, pp 1375-1377,

[6] R.L.Russel, and K.H.Norsworthy, “Eddy current and wall losses in screened-rotor induction motors” Proc. IEE, 1958, 105A. pp 163-175.

[7] E.M.Freeman, “Travelling waves in induction machines: input impedance and equivalent circuits.” Proc. IEE, vol. 115, No 12, December 1968, pp 1772-1776.
[8] J.H.H.Alwash, and J.F.Eastham, “Permeance harmonic analysis of short-stator machines." Proc. IEE, Vol. 123, No. 12, December 1976, pp 1335-1340.
[9] M.J.Balchin, and J.F.Eastham, “Performance of linear induction motors with air gap windings.” Proc. IEE, vol. 122, No.12, December.1975, pp 1382-1389.
[10] MEGA V6.24 User Manual Applied Electromagnetic Research Centre Bath University

Appendix

Test motor details

Number of poles = 12
Slots per pole and phase = 2
Pole pitch = 0.105m
Primary stack width = 0.084m
Width of the secondary conductive plate = 0.188m
Depth of the secondary conductive plate = 0.005m
Resistivity of the secondary conductive plate at ambient temperature = 3.05E-08 Ohm.m
Number of turns per coil = 14

Permanent magnet unit details

Magnet length = 0.06m
Magnet thickness = 0.005m
Magnet width = 0.0825 m
Magnet remanence = 1.12T
Secondary plate width = 0.188m
Secondary plate thickness = 0.005m
Secondary plate resistivity at ambient temperature = 3.05E-08 Ohm.m
Pole pitch = 0.0805m

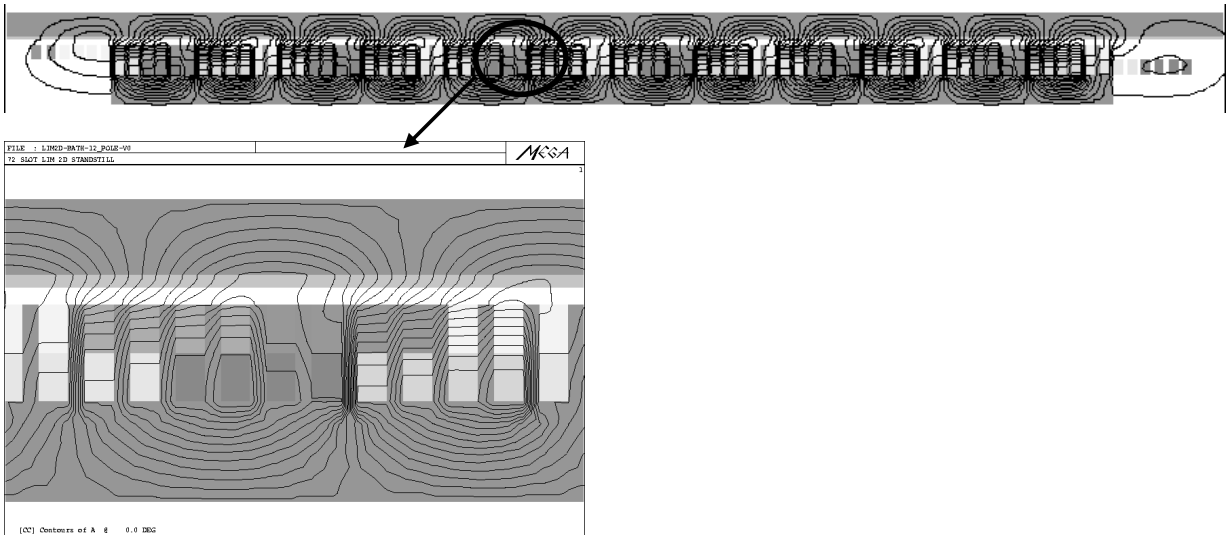

Figure 10 2D finite element flux plot

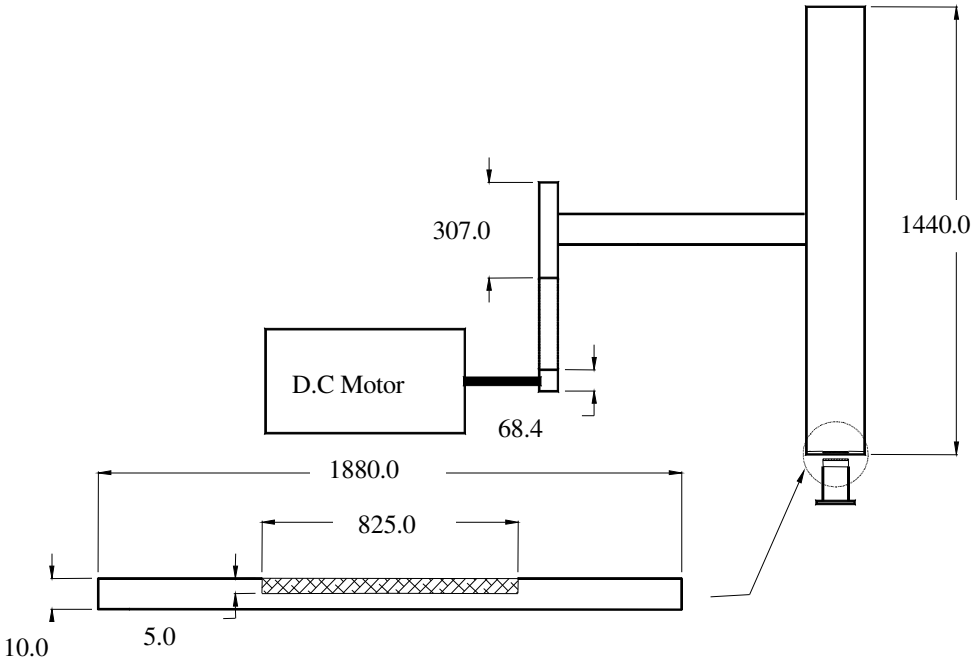

Figure 11 Experimental test rig

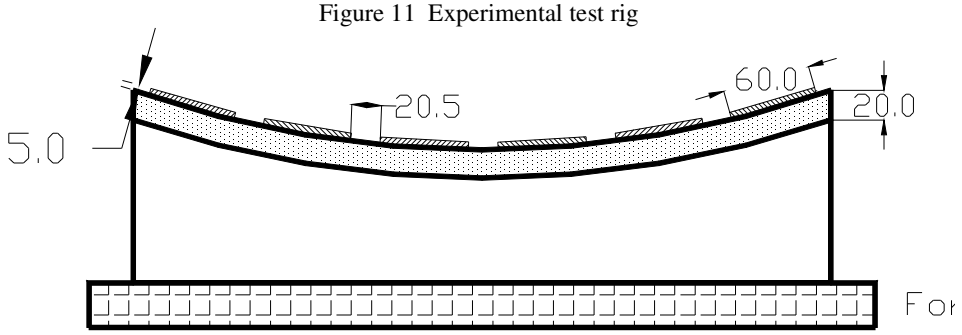

Figure 12 Permanent magnet unit